Article

Power Optimization Control Scheme for Doubly Fed Induction Generator Used in Wind Turbine Generators

Darya Khan [1], Jamshed Ahmed Ansari [1,2,*], Shahid Aziz Khan [2] and Usama Abrar [2]

[1] Department of Electrical Engineering, Sukkur IBA University, Sukkur 65200, Pakistan; darya.khan@iba-suk.edu.pk

[2] School of Electrical and Electronic Engineering, North China Electric Power University, Beijing 100085, China; shahidazizkhan1@gmail.com (S.A.K.); uabrar@gmail.com (U.A.)

* Correspondence: Jamshed.ahmed@iba-suk.edu.pk

check for updates

Abstract: Scientists and researchers are exploring different methods of generating and delivering electrical energy in an economical and reliable way, enabling them to generate electricity focusing on renewable energy resources. All of these possess the natural property of self-changing behavior, so the connection of these separate independent controllable units to the grid leads to uncertainties. This creates an imbalance in active power and reactive power. In order to control the active and reactive power in wind turbine generators with adjustable speed, various control strategies are used to allay voltage and current variations. This research work is focused on the design and implementation of effective control strategies for doubly fed induction generator (DFIG) to control its active and reactive power. A DFIG system with its control strategies is simulated on MATLAB software. To augment the transient stability of DFIG, the simulation results for the active and reactive power of conventional controllers are compared with three types of feed forward neural network controllers, i.e., probabilistic feedforward neural network (PFFNN), multi-layer perceptron feedforward neural network (MLPFFN) and radial basic function feedforward neural network (RBFFN) for optimum performance. Conclusive outcomes clearly manifest the superior robustness of the RBFNN controller over other controllers in terms of rise time, settling time and overshoot value.

Keywords: artificial intelligence; feedforward neural network; power system stability; vector control; wind turbine generator

---

1. Introduction

Electrical energy and electrical power systems frameworks play vital roles in the economic development of a country [1,2]. The actual worry for researchers and system engineers is to lessen misfortunes, and change the execution and reduce the unit cost of generated power [3,4]. Traditional ways to generate electricity rely on gas, oil and coal, which are sparse means [3,5]. Power originating from these assets is very costly, and the lingering of these solutions has a harmful impact on wellbeing as well as polluting the earth [6]. A superior choice is to switch to sustainable assets like sun photovoltaic, biogas energy sources and wind power generation [5,6].

Wind turbines are thought to be a probable wellspring of electrical energy in the near future [7]. The wind turbines are subjected to both sessions, i.e., compulsion and changing wind behavior [4,5,7,8]. Normally, the performance of a traditional control mechanism is satisfactory, but problems arise when the wind speed changes or machine parameters vary, so the overall output power being contributed to the main grid should be a stabilized one [5,9,10]. A control mechanism must have a few components in order to limit the control catch at excessive speeds so as to stop overloading [3,5,7,11]. Variable

speed turbines provide smart controllability and are capable of generating power at the megawatt scale [3,12,13]. These systems are equipped with a DFIG generator. The variable speed turbine can tolerate some of the power variation due to turbulence by increasing the rotor speed, so that the power output at each wind speed can be controlled [14–16].

In the literature review, two main control strategies are adopted to achieve optimal power stabilization of the DFIG, i.e., the vector control (VC) and direct torque control (DTC), to augment the machine realization [4]. DTC is a non-linear type of control that functions in a hysteresis style. It detects the nonlinear parameters of machines such as flux and torque, and adjusts the rotor voltage to a suitable power [3,10,17,18]. Another scheme for linear control, named vector control (VC), depends on simple single input, single output feedback type regulators, i.e., PI and PID controllers, or a more progressive state space concept. This approach leads to the conversion of a complex moveable rotating frame into an equivalent orthogonal two-dimensional stationary DQ frame [19–23]. So, to make the parameter approximation simpler, this work is categorized in vector control schemes. A summarized chart for the control schemes discussed in the literature review is shown in Figure 1.
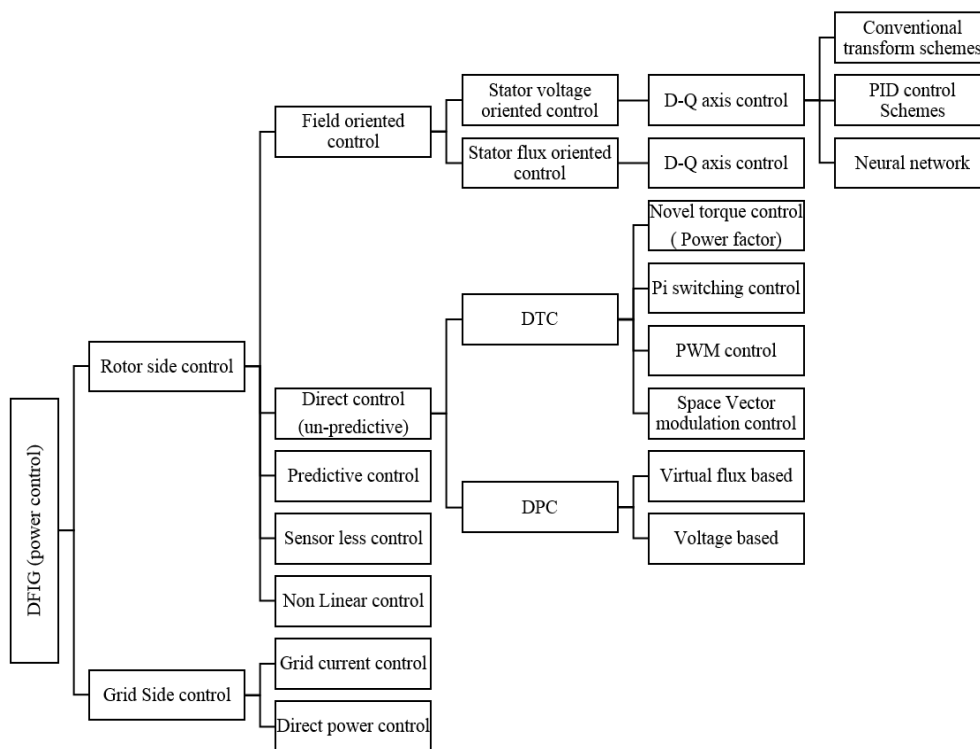

Figure 1. Power control schemes discussed in literature review.

This article simulates the mathematical model of the DFIG-equipped wind turbine. For maximum performance, traditional performance controllers are compared with three types of feedforward neural network-based controllers. The frequently used rotor-side control scheme adapts bidirectional AC-AC sequential control converters so as to maintain steady rotor power recovery. The VC scheme is used to attain immediate and decoupled control of the machine by regulating rotor currents. The related work is classified into linearized control schemes so that rotating complex three-phase parameters (voltage and current) are remolded to corresponding static DQ reference frames. In this way, the synchronous d–q reference frame rotates at angular speed. The rest of the paper is organized as follows: Section 2 discusses the methodology for the development of DFIG and the proposed controllers, Section 3 presents the software implementation of the model, results are discussed in Section 4 and finally Section 5 concludes the paper.

2. Methodology

2.1. Active and Reactive Power Control

Active power control is considered as a series of regulating process between machine and turbine; if wind speed is sufficient then a power controller regulates the pitch angle of the blades to get the maximum amount of torque required to generate maximum power. This machine may enable the decoupled control of actual and reactive power; the actual power is associated with mechanical torque, and is thus related to the electrical speed of the generator, so for that many studies have been performed.

In order to obtain a natural response using the default parameters of machines, a simplified approach is adopted by neglecting stator side impedance Rs, JXis and JXir. Thus the stator and rotor powers per phase can be represented as [24]:

$$S_s = V_s I_s = P_s + JQ_s \tag{1}$$

$$S_r = V_r I_r = P_r + JQ_r \tag{2}$$

where Equation (1) shows apparent power at stator side and Equation (2) represents apparent power at rotor side.

Considering that the turns ratio between stator and rotor is unified, the new rotor voltage V_r' and new rotor current I_r' can be expressed as:

$$V_r' = V_r \text{ and } I_r' = I_r$$

Taking the complex conjugate of stator current and multiplying it with stator voltage will give the power equation at stator side:

$$V_s I_s^* = |I_r'|^2 R_r'/s + J|V_s^2|/X_m + V_r' I_r'^*/s \tag{3}$$

Taking real and imaginary parts, we can calculate active and reactive power:

$$P_s = |I_r'|^2 R_r'/s - \text{Re}[V_r I_r^*]/s = |I_r'|^2 R_r'/s - P_r/s \tag{4}$$

$$Qs = |V_s^2|/X_m - I_m[V_r I_r]/s = |V_s^2|/X_m - Q_r/s \tag{5}$$

DFIG has the ability to amplify the rotor power via power converters, and the desired speed scale of the generator directly depends upon the R_{SC} of the power converter, i.e., for the DFIG having a speed range of ±0.3 slip, the power converters must be 30% of the machine's ratings.

2.2. d-q Vector Control

According to the flux reference frame of the stator, simplified equations representing the dynamics of the induction machine are given by [24]:

$$^r V_s = R_s{}^r i_s + \frac{d^r \lambda_s}{dt} + j\omega_k{}^r \lambda_s \tag{6}$$

where ωK is the angular speed of the stator flux reference frame; the voltage equations at the rotor are not as important because the rotor side is current-controlled, and the rotor current space vectors are derived from the grid, so are already determined. The stator flux reference frame refers to a frame with a d-axis aligned along the stator flux space vector, so can be expressed as:

$$^r \lambda_s = \lambda_{ds}; \ \lambda_{qs} = 0 \tag{7}$$

Substituting Equation (6) in to (7), to express them in d and q components,

$$V_{ds} = R_s i_{ds} + \frac{d\lambda_s}{dt} \tag{8}$$

$$V_{qs} = R_s i_{qs} + \omega_k \lambda_k \tag{9}$$

But as we know

$$^r\lambda_s = L_s{}^r i_s + L_m{}^r i_r \tag{10}$$

In terms of rotor current and stator flux, the stator d–q components can be represented as:

$$i_{qs} = -\left(\frac{L_m}{L_s}\right) i_{qr} \tag{11}$$

$$i_{ds} = -\left(\frac{L_m}{L_s}\right) i_{dr} - \lambda_s \tag{12}$$

The dynamics of the induction machine are given by:

$$\frac{d\lambda_s}{dt} = V_{ds} - \frac{R_s}{L_s}(\lambda_s - L_m i_{dr}) \tag{13}$$

The above Equations (12) and (13) can be solved to get the stator flux linkage variations. Equation (14) is used to calculate the angular velocity of the stator flux used in the inter-conversion from abc to d–q transformations. since λqs = 0, the electromagnetic torque produced by the machine would be:

$$T_e = -\left(\frac{L_m}{L_s}\right) \lambda_s i_{qr} \tag{14}$$

So stator flux is supposed to be controlled through the d-component of the rotor current, and the torque produced can be controlled by the *q*-axis component of the rotor. To achieve control over stator voltages and rotor current, the flux of the rotor and the torque of the machine should be properly supervised and controlled.

2.3. Implementation of Probabilistic Feedforward Neural Network

A PFFNN is categorized under the category of a feed-forward neural network. In this research work, to control and achieve stability and consistency in the active and reactive performance of a DFIG, a PFFNN controller has been developed in the MATLAB Neural Network Toolbox. This is a supervised workout. Prior to the implementation of PFFNN, the conventional PID controller is implemented in MATLAB, with the values for which the response from DFIG was satisfactory used as input and training data for the PFFNN. After generating a neural network containing these responses to the DFIG model, this newly-born file runs in conjunction with the PID controller in order to set the responses. Initially, these PFFNNs work in a similar way to PID, as it is part of the training [25]. Once training is completed, this controller can now be replaced with PI and PID for DFIG power control. The trained controller provides better performance over a wide range of disturbances.

The PFFNN is prepared with an overseen/monitored preparing procedure of artificial neural networks [25]. In this article, PFFNN is created as a unique sort of trained and ingenious controller. The input and target data for preparing the PNN are acquired from the input and output of the ordinary controller [25]. The layers, weights and biases of the simulated PFFNN network are shown in Figures 2 and 3 respectively.

2.4. Implementation of Multi-Layer Perceptron Feedforward Neural Network

An MLP has been prepared with the LEVENGBERG-MARQURADT Back progression (BP) learning algorithm, which depends on the supervised learning of ANN. This algorithm is faster as

compared to others. In this work, the network is prepared to act as an extraordinary sort of a traditional controller. The sources of information and target information for the preparing of the neural system are made from the current data (inputs and yield) of that controller in a closed loop connected in parallel with plant [26]. The model is reproduced and the PID controller is utilized as a mentor for the system in the preparation/training procedure. The subsequent system has designed to carry on in a style indistinguishable from its coach so that it can perform well in that particular condition.
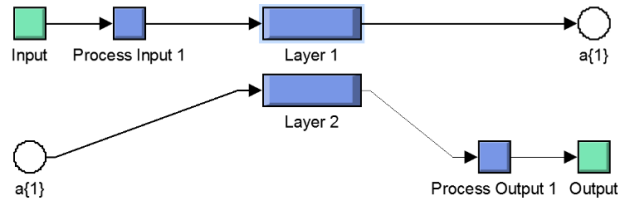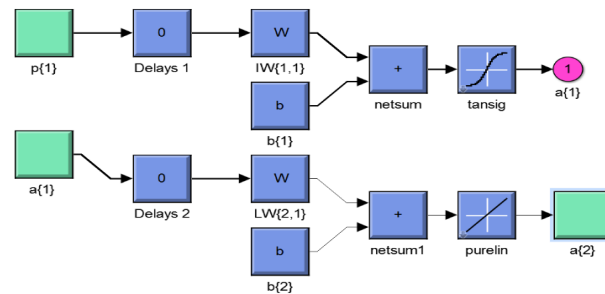

Figure 2. Layers of PFFNN.

Figure 3. Weights and biases of PFFNN.

In this investigation, an MLP arrangement is made which gives a competent performance. The approach depends on the supervised learning of a neural system, so information for the preparing must be approximated. For this reason, three contributions are recorded at the PID approaching sign and one output flag active from PID. The three inputs of the PID controller are connected as an input to the information layer of the MLP neural system. Active and reactive power are the two required outputs for the proposed network. The layers of simulated MLPFFNN are shown in Figure 4.
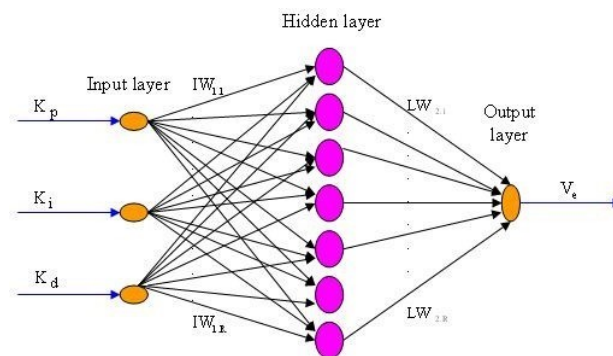

Figure 4. Layers of MLPFFNN.

2.5. Implementation of Radial Basic Function Neural Network

The RBF network is developed here for power system stabilization of the DFIG generator. There are no strict standards for choosing a specific number of neurons in the hidden layer of the RBF to arrange for a particular application. Then, again, neurons in the concealed layer are made by themselves. An orthogonal least square (OLS) calculation consequently picks an appropriate number of neurons in the hidden layer of the RBF network from the input data.

The RBF is used to approximate a function. The neurons are added to the hidden layer until the specified mean square error goal is met. For the training of the RBF network, the input vector is found with the greatest error. A radial based transfer function neuron is added with weights equal to the vector of step 2. The linear transfer function layer weights are redesigned to minimize error. It is found that 25 neurons are created in the hidden layer. One neuron or node with a linear transfer function is used in the output layer. The spread constant is set at 1.5. The simulated RBF network and its layers are shown in Figures 5 and 6, respectively.
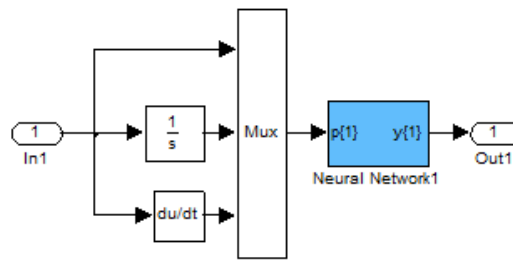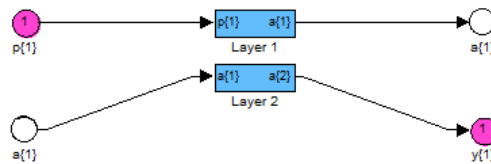

Figure 5. Simulated RBF network.

Figure 6. Layers of RBF network.

3. Implementation of DFIG with Its Controllers in MATLAB/Simulink

Figure 7 represents the implantation of a simplified mathematical model of DFIG in the MATLAB Simulink tool, taking into account the synchronized d–q reference frame. This model represents the total system components (parameters) needed to run the simulation. The transfer function block diagram for DFIG is shown in Figure 8.
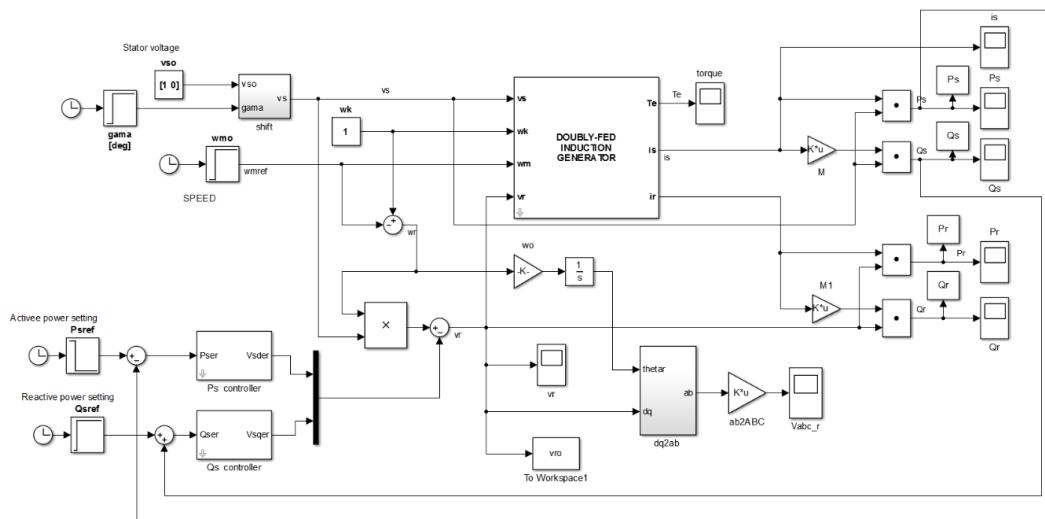

Figure 7. Simulated DFIG along with its control schemes.

Operating Conditions for Model

For the DFIG machine connected with a wind turbine, assumptions of data and parameters are made according to IEEE standards, with an external resistance of 0.02 p.u. and inductance of 0.1 p.u. the operating parameters for the simulation model are shown in Table 1 [1].
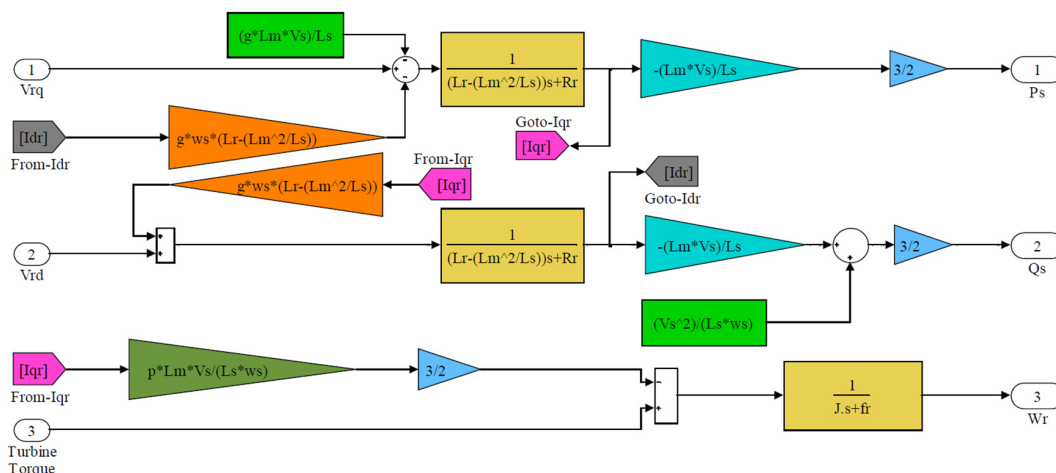
Figure 8. Transfer functions of simulated DFIG.

Table 1. Operating parameters for simulation model.

Quantity	Value
Active power (P)	1.0 p.u
Reactive power (Q)	0.62 p.u
Load power factor (p.f)	0.85 p.u
Stator Voltage (V_t)	1.0 p.u
Stator Resistance (Rs)	0.01 p.u
Stator Leakage inductance	0.1 p.u
Rotor Resistance(Rr)	0.02 p.u
Magnetizing Inductance (Lm)	5 p.u
Base frequency (ω_R) Radians/s	314.28
Damping value (D)	0.8
Inertia value (H)	4
Reference voltage (V_{Ref})	1 p.u
Sensor gain (K_R)	1
DFIG Linear Parameters	
K_1	1.0075
K_2	1.0578
K_3	−0.0409
K_4	0.4971
Active Power Controllers Parameters	
Washout network Saturation	10
Lead–lag network	$\tau_1 = 0.100$, $\tau_2 = 10.00$
Lag–lead network	$\tau_3 = 0.100$, $\tau_4 = 10.00$
Reactive Power Controllers Parameters	
Washout network Saturation	1000
Lead–lag network	$\tau_1 = 0.100$, $\tau_2 = 10.00$
Lag–lead network	$\tau_3 = 0.100$, $\tau_4 = 10.00$
PID Parameters	
Proportional gain (Kp)	0.1
Integral gain (Ki)	10
Derivative gain (Kd)	0.1

4. Results and Discussion

The simulation results for the active and reactive power at the stator and rotor sides of the DFIG with different FFNN controllers are discussed in the following.

4.1. Response for Active Power at Stator

The response of the DFIG generator with PI, PID, PFFNN, MPLFFNN and RBFFNN controllers at prescribed gains and the above-mentioned assumptions, along with certain parameters and a stator side active power controller, is shown in Figure 9.
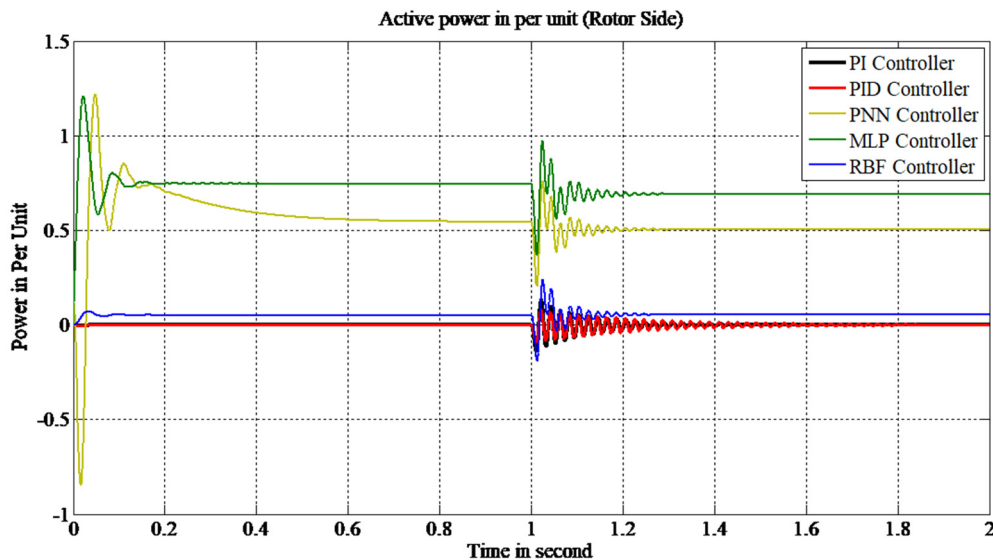

Figure 9. Active power at stator.

At normal loading conditions, the results for the active power at the stator of the DFIG clearly show that the RBFFNN controller is more suitable and applicable than PID and conventional controllers, as it improves the efficiency of the DFIG. Table 2 compares the responses of DFIGs equipped with different power controllers as regards step input, and the performance of the controllers is evaluated on the basis of overshoot, rise time and settling time.

Table 2. Active power at stator side.

S. No.	Type of Controller	Overshoot in p.u.	Settling Time in Seconds	Rise Time in Seconds
1	PI	0.378	1.9	0.13
2	PID	0.26	2	0.11
3	PFFNN	1.3	1.38	0.015
4	MLPFFN	1.2	1.36	0.013
5	RBFFFN	0.38	1.33	0.010

From Table 2, it can be observed that the overshoot value with a conventional control scheme is 0.378 p.u., while for PID it is 0.260 p.u., and it is highest with PNN and MLP controllers with overshoot values of 3 and −1.2 p.u., respectively. It is lowest with the RBF-based power controller, with a value of 0.38 p.u. For settling time, PI and PID took more than 1.9 and 2 s, respectively, while PNN took 1.38 s to settle. The RBF- and MLP-based power controllers have settling times of 1.36 and 1.33 s, respectively. So, with these observations, the above table clearly suggests the RBF-based power controller as an effective controller for active power control at the stator side, with a lower settling time, a lower rise time and a reduced overshoot value.

4.2. Response for Reactive Power Control at Stator

The response of the DFIG generator at prescribed gains and with the above-mentioned assumptions, along with certain parameters and stator side reactive power determined by different controllers, is shown in Figure 10.
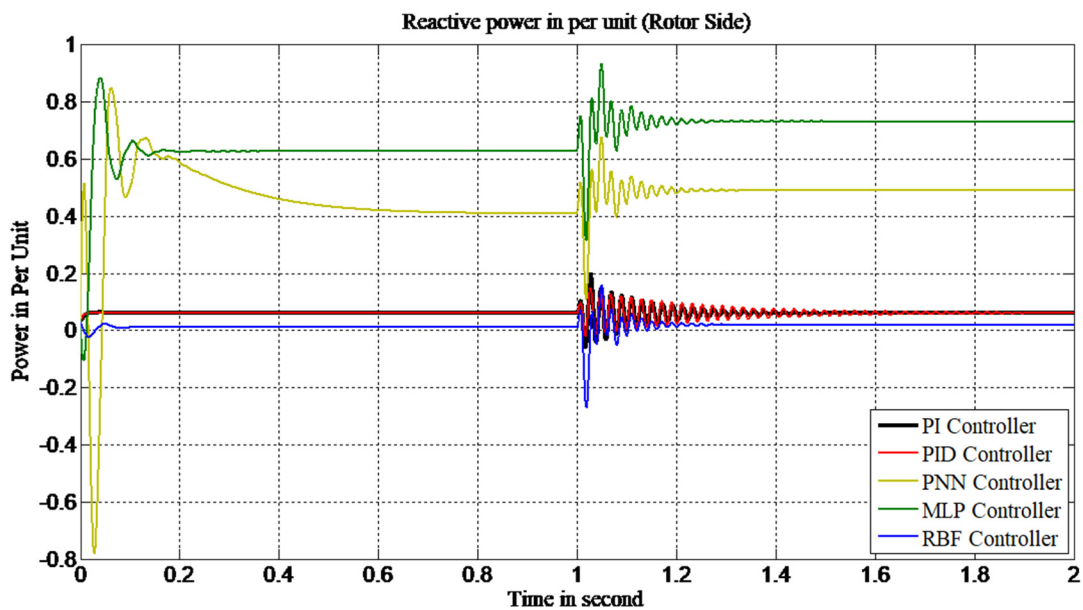
Figure 10. Reactive power at stator.

Under normal loading conditions, the results for the reactive power at the stator of the DFIG clearly show that feedforward neural network (FFNN)-based controllers are more suitable and applicable than PID and conventional controllers, and they improve the efficiency of DFIG. An FFFN-based power controller has a better effect on the reactive power at the stator of the DFIG. Table 3 compares the responses of the DFIG equipped with different power controllers.

Table 3. Reactive power at stator side.

S. No	Type of Controller	Overshoot in p.u.	Settling Time in Seconds	Rise Time in Seconds
1	PI	0.376	1.8	0.15
2	PID	0.257	2	0.13
3	PFFNN	0.84	1.48	0.017
4	MLPFFNN	0.8	1.37	0.015
5	RBFFNN	0.18	1.3	0.011

It can be observed from Table 3 that the overshoot values of PI and PID are 0.376 and 0.257 p.u., respectively, while PNN and MLP have values of 2.4 and 0.8 p.u., respectively. The RBF-based power control has an overshoot value of 0.18 p.u., which is the least among them all. The rise time and settling time with the RBF controller are also the lowest among all the controllers. With the above observations, it can be concluded that RBF is more suitable and applicable than the other types of controllers, and it improves the efficiency of power system.

4.3. Response for Active Power Control at Rotor

The response of the DFIG generator at prescribed gains and with the above-mentioned assumptions, along with certain parameters of the stator side reactive power controller, is shown in Figure 11.
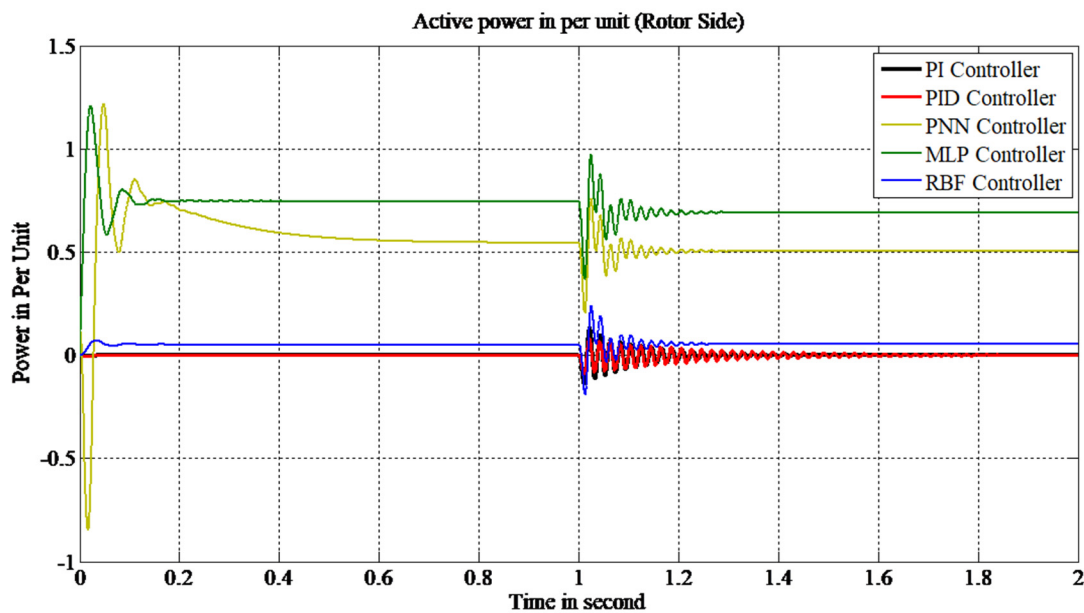
Figure 11. Active power at rotor.

Under normal loading conditions, the results for the active power at the rotor of the DFIG clearly show that FFNN controllers are more suitable and applicable than PID and conventional controllers. Table 4 compares the responses of DFIGs equipped with different power controllers for active power at the rotor side.

Table 4. Active power at rotor side.

S. No.	Type of Controller	Overshoot Value in p.u.	Settling Time in Seconds	Rise Time in Seconds
1	PI	0.134	1.78	0.17
2	PID	0.08	2	0.15
3	PFFNN	1.23	1.47	0.015
4	MLPFFNN	1.2	1.36	0.013
5	RBFFFNN	0.22	1.34	0.011

It can be observed in Table 4 that the overshoot values of PI and PID are 0.134 and 0.08 p.u., respectively. However, with FFNN controllers, the PNN has a value 1.23, MLP has a value of 1.2 and the RBF-based power controller has an overshoot value of 0.22 p.u., which is the lowest among the other FFNN controllers. For settling time, PI and PID took 1.78 and 2 s, respectively, while PNN took 1.47 s to settle, but RBF and MLP have settling times of 1.36 and 1.34 s, respectively. With the above observations it can be concluded that the RBF-based power control is more suitable and applicable than other types of controllers, as it improves the efficiency of the power system, and reduces settling time and rise time. However, the RBF controller possesses a slightly higher overshoot value than conventional controllers, but it achieves very quick stabilization, and is supposed to be more cognitive about systems dynamics, thus its performance in active power control is better as compared to other controllers.

4.4. Response for Reactive Power Control at Rotor

The response of a DFIG generator at prescribed gains and with the above-mentioned assumptions, along with certain parameters of the rotor side reactive power controller, is shown in Figure 12.
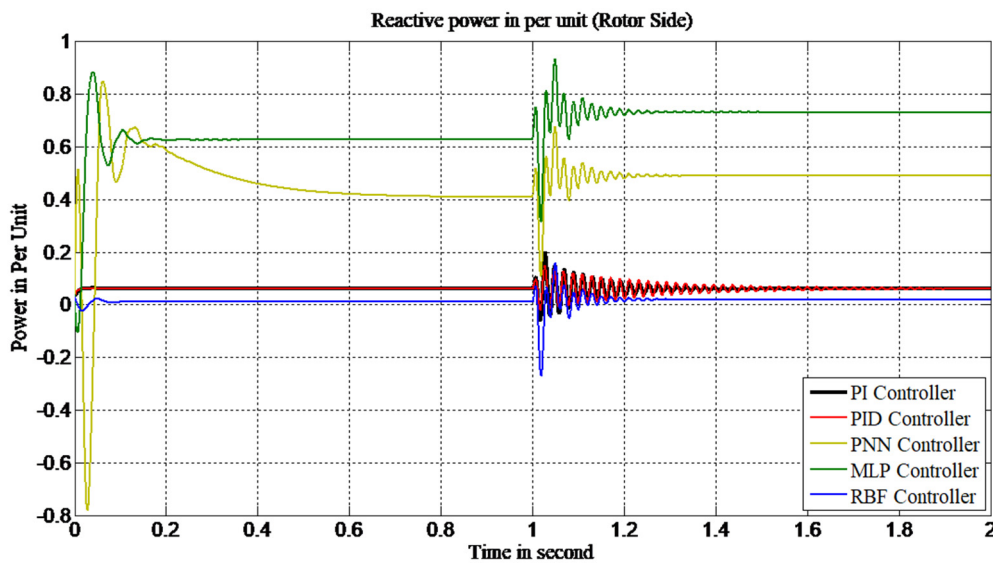
Figure 12. Reactive power at rotor.

Given the above results, it can be observed that among all other conventional and FFNN controllers, RBF shows the better response. Table 5 compares the response of DFIG equipped with different power controllers with regard to step input.

Table 5. Reactive power at rotor side.

S. No.	Type of Controller	Overshoot in p.u.	Settling Time in Seconds	Rise Time in Seconds
1	PI	0.19	1.78	0.15
2	PID	0.15	2	0.14
3	PFFNN	0.86	1.43	0.017
4	MLPFFNN	0.93	1.36	0.014
5	RBFFFNN	0.15	1.32	0.011

It can be observed from Table 5 that the overshoot value of the conventional control scheme is 0.19 p.u., and with PID it is 0.15 p.u., while with PNN and MLP the values are 0.86 and 0.93 p.u., respectively. With the RBF-based power controller this value is 0.15 p.u. The overshoot values for the RBF and PID controllers are the same, and are lower than all other controllers. However, the RBF-based controller also possesses lower settling and rising times than all other controllers. As such, with the above observation it can be clearly stated that the RBF-based power controller offers robust control of the reactive power at the rotor side.

From the detailed discussion of the results presented, it is clear that the performance of the RBF network is better than conventional and other FFNN controllers. The RBF have favorable characteristics, including the best approximation property and a compact network structure. The RBF networks possess a faster training time than networks. An RBF-based power controller has a better effect on the terminal voltage, reactive power, rotor current and reference DC voltage, and system stability can be achieved in a very short time span with a much lower number of offshoots or ripples. As compared to other power regulators, it can achieve very quick stabilization and is supposed to be more cognitive about systems dynamics, and its performance in terms of terminal voltage and reactive power control is better as compared to other controllers. However, this type of controller needs a complex algorithm for non-linear systems, which increases the computational burden. The training of RBF is faster than other FFNN controllers, but classification is slow. This is due to the fact that every hidden layer in the RBF network has to compute the RBF function for every input vector.

5. Conclusions

In this research work, the DFIG-based wind turbine generator is modeled in MATLAB and the VC scheme has been executed. This technique is used to decouple the active and reactive power exchanged between the stator and the grid. To alleviate the unwanted power fluctuations, suitable regulators with suitable power gains are implemented. The proposed RBFFNN controllers for the DFIG have been effectively tested, as a major aspect of the VC transformation, to interpret the rotor-side power gains. This provides the promising and vigorous execution of the proposed control scheme.

This type of controller can effectively control the oscillations at the stator and rotor side of the DGIF. However, in the future, non-linear modeling will be required due to the non-linear behavior of the input and output signals of a system (DFIG) subjected to uncertain input patterns, such as wind.

Author Contributions: Conceptualization, D.K. and J.A.A.; methodology, D.K.; software, D.K.; validation, S.A.K.; formal analysis, U.A.; writing—original draft preparation, D.K., J.A.A, S.A.K. and U.A.; writing—review and editing, J.A.A. All authors have read and agreed to the published version of the manuscript.

Conflicts of Interest: The authors declare no conflict of interest.

References

1. Deshmukh, M.K.; Moorthy, C.B. Review on stability analysis of grid connected wind power generating system. *Int. J. Electr. Electron. Eng. Res. Dev. IJEEERD* **2013**, *3*, 1–33.
2. Duong, M.Q.; Leva, S.; Mussetta, M.; Le, K.H. A Comparative Study on Controllers for Improving Transient Stability of DFIG Wind Turbines during Large Disturbances. *Energies* **2018**, *11*, 480. [CrossRef]
3. Pichan, M.; Rastegar, H.; Monfared, M. Fuzzy-based direct power control of doubly fed induction generator-based wind energy conversion systems. In Proceedings of the 2012 2nd International e Conference on Computer and Knowledge Engineering (ICCKE), Mashhad, Iran, 18 October 2012; pp. 66–70.
4. Abdel-Khalik, A.S.; Elserougi, A.; Massoud, A.; Ahmed, S. A power control strategy for flywheel doubly-fed induction machine storage system using artificial neural network. *Electr. Power Syst. Res.* **2013**, *96*, 267–276. [CrossRef]
5. Tuka, M.B.; Leidhold, R.; Mamo, M. Modeling and control of a Doubly Fed Induction Generator using a back-to-back converters in grid tied wind power system. In Proceedings of the 2017 IEEE PES PowerAfrica, Accra, Ghana, 27–30 June 2017; pp. 75–80.
6. Wang, L.; Wang, K.-H. Dynamic Stability Analysis of a DFIG-Based Offshore Wind Farm Connected to a Power Grid through an HVDC Link. *IEEE Trans. Power Syst.* **2010**, *26*, 1501–1510. [CrossRef]
7. Yousefi-Talouki, A.; Pouresmaeil, E.; Jorgensen, B.N. Active and reactive power ripple minimization in direct power control of matrix converter-fed DFIG. *Int. J. Electr. Power Energy Syst.* **2014**, *63*, 600–608. [CrossRef]
8. Vittal, E. The Impact of Reactive Power from Wind Generation on Power System Stability. Ph.D. Thesis, University College Dublin, Dublin, Ireland, September 2011.
9. Luna, A.; Lima, F.; Santos, D.; Rodriguez, P.; Watanabe, E.H.; Arnaltes, S. Simplified Modeling of a DFIG for Transient Studies in Wind Power Applications. *IEEE Trans. Ind. Electron.* **2010**, *58*, 9–20. [CrossRef]
10. Yang, X.; Liu, G.; Li, A.-P.; Van Dai, L. A Predictive Power Control Strategy for DFIGs Based on a Wind Energy Converter System. *Energies* **2017**, *10*, 1098. [CrossRef]
11. Teng, W.; Meng, Y. An improved control strategy to the frequency regulation of DFIG based wind turbine. *J. Renew. Sustain. Energy* **2017**, *9*, 63303. [CrossRef]
12. Kaloi, G.S.; Wang, J.; Baloch, M.H. Active and reactive power control of the doubly fed induction generator based on wind energy conversion system. *Energy Rep.* **2016**, *2*, 194–200. [CrossRef]
13. Nora, Z.; Hocine, L. Active and Reactive Power Control of a Doubly Fed Induction Generator. *Int. J. Power Electron. Drive Syst. IJPEDS* **2014**, *5*, 244–251. [CrossRef]
14. Tohidi, S.; Mohammadi-Ivatloo, B. A comprehensive review of low voltage ride through of doubly fed induction wind generators. *Renew. Sustain. Energy Rev.* **2016**, *57*, 412–419. [CrossRef]

15. Bhutto, D.K.; Ansari, J.A.; Chachar, F.; Katyara, S.; Soomro, J. Selection of optimal controller for active and reactive power control of doubly fed induction generator (DFIG). In Proceedings of the 2018 International Conference on Computing, Mathematics and Engineering Technologies (iCoMET), Sukkur, Pakistan, 3–4 March 2018; pp. 1–5.

16. Duggirala, V.N.A.; Gundavarapu, V.N.K. Dynamic Stability Improvement of Grid Connected DFIG Using Enhanced Field Oriented Control Technique for High Voltage Ride Through. *J. Renew. Energy* **2015**, *2015*, 1–14. [CrossRef]

17. Bouchiba, N.; Barkia, A.; Sallem, S.; Chrifi-Alaoui, L.; Drid, S.; Kammoun, M.B.A. Implementation and comparative study of control strategies for an isolated DFIG based WECS. *Eur. Phys. J. Plus* **2017**, 132. [CrossRef]

18. Dong, J.; Li, S.; Wu, S.; He, T.; Yang, B.; Shu, H.; Yu, J. Nonlinear Observer-Based Robust Passive Control of Doubly-Fed Induction Generators for Power System Stability Enhancement via Energy Reshaping. *Energies* **2017**, *10*, 1082. [CrossRef]

19. Vahdati, P.M.; Vanfretti, L.; Amini, M.H.; Kazemi, A. Hopf Bifurcation Control of Power Systems Nonlinear Dynamics Via a Dynamic State Feedback Controller—Part II: Performance Evaluation. *IEEE Trans. Power Syst.* **2017**, *32*, 1. [CrossRef]

20. Njiri, J.G.; Söffker, D. State-of-the-art in wind turbine control: Trends and challenges. *Renew. Sustain. Energy Rev.* **2016**, *60*, 377–393. [CrossRef]

21. Sun, T.; Chen, Z.; Blaabjerg, F. Transient stability of DFIG wind turbines at an external short-circuit fault. *Wind. Energy* **2005**, *8*, 345–360. [CrossRef]

22. Prabha, M.; Priyadharshini, M.; Priyanga, P.M.; Shanmugapriya, K. Modeling of Doubly Fed Induction Generator with Low Voltage Ride through Mechanism. *Int. J. Adv. Res. Electr.* **2017**, *6*. [CrossRef]

23. Gupta, A.; Singh, S.N.; Khatod, D.K. Modeling and simulation of doubly fed induction generator coupled with wind turbine-an overview. *J. Eng. Comput. Appl. Sci.* **2013**, *2*, 45–54.

24. Petersson, A. Analysis, Modeling and Control of Doubly-Fed Induction Generators for Wind. Ph.D. Thesis, Chalmers University of Technology, Gothenburg, Sweden, 2005.

25. Ansari, J.A.; Memon, A.P.; Shah, M.A. Probabilistic Feedforward Neural Network Based Power System Stabilizer for Excitation Control System of Synchronous Generator. *Bahria Univ. J. Inf. Commun. Technol. BUJICT* **2015**, *8*, 70–74.

26. Bhutto, D.K.; Ansari, J.A.; Bukhari, S.S.H.; Chachar, F.A. Wind energy conversion systems (WECS) generators: A review. In Proceedings of the 2019 2nd International Conference on Computing, Mathematics and Engineering Technologies (iCoMET), Sukkur, Pakistan, 30–31 January 2019; pp. 1–6.